

Modeling Fluid Flow and Heat Transfer in Shell and Tube Heat Exchangers According to Shape and Layout of Tubes

Mehdi Salmanzadeh

Department of Mechanical Engineering ,Islamic Azad
University, Shoushtar Branch,
Shoushtar, Iran
Mehdi2852003@gmail.com

Mohamad Reza Isvandzibaei

Department of Mechanical Engineering ,Islamic Azad
University, Andimeshk Branch,
Andimeshk, Iran
esvandzebaei@yahoo.com

Abstract—Although typical shell and tube heat exchangers (STHE) have a long-standing history and several achievements in the industry, accounting for the majority of new exchangers in refinery, petrochemical and power plants, these equipment have operational problems and limitations. Small shell-side heat transfer coefficient in these exchangers increases the possibility of dead zone creation, and settling in them. In addition, pressure drop is high relative to the heat transfer coefficient and vibration of the tube bundle. In this study, circular and elliptical tubes, and their layout in the exchanger were investigated. Proper placement of tubes in exchangers eliminates simple STHE associated problems. Simple tubes in heat exchangers produce vibration, reduce heat transfer, and increase settling and corrosion relative to the tubes with square or elliptical layout patterns. The majority of these problems are solved through designing tubes with triangular pitch or using elliptical tubes. Laws governing heat transfer reveal the advantage of using elliptical tubes or a certain layout. Fluent outputs were compared to the findings of previous studies and the most optimum layout was proposed.

Keywords-component; Heat Exchanger, Shell and Tube, Triangular Pitch, Square Pitch

I. INTRODUCTION (HEADING 1)

The STHEs account for approximately 80% of all new exchangers in refinery, petrochemical, and power plants. These exchangers are applicable to a wide range of pressure and temperature, which can be extended by new designs. Despite having several undeniable advantages, other types of heat exchangers, such as plate and frame heat exchangers, operate only at pressure < 16bar and temperature < 200°C; therefore, this subject has attracted much attention to find advanced solutions to cope with current design deficiencies [1].

Baffling in shell-side TEMA STHE not only keeps the tube bundle fixed in place, but also generates a cross flow. This zigzag movement wastes energy during flow diversion, instead of increasing heat transfer coefficient in the shell-side. This phenomenon also causes fluid leakage from the tube nuzzles, baffle, and shell, resulting in cross flow reduction. In addition, baffles result in the creation of dead zones, reduce heat transfer, and increase settling and corrosion [2]. The mean thermal difference or thermal efficiency is comparable in STHEs with the assumption of the presence of perfect radial mixing and the lack of axial

mixing. In practice, the axial mixing is larger in exchangers with baffle, and this effect is intensified by leakage and bypass flows in the tube bundle, which are partially involved in heat transfer.

The advantages of elliptical heat exchangers and/or exchangers with tubes with triangular pitches were compared with tubes with square pitches. The advantages of each layout relative to the other were calculated and investigated with Fluent [3].

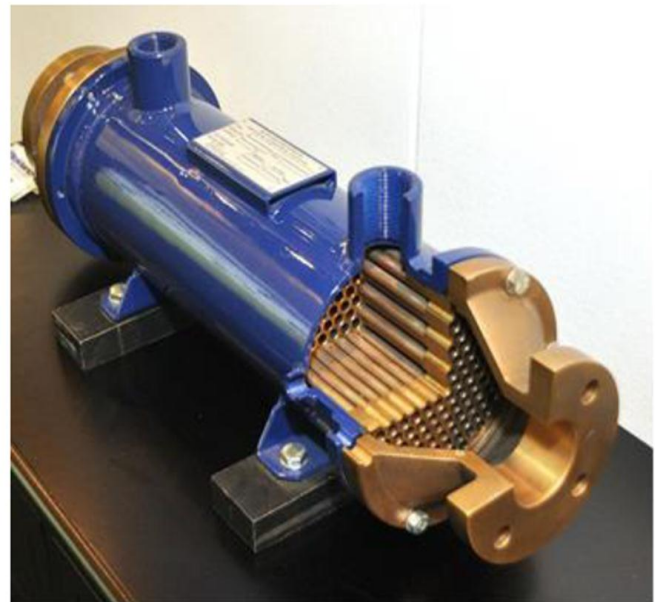


Figure 1. Sketch of segmental cut of semi-industrial prototype of a shell and tube exchanger

II. EXCHANGER TUBE LAYOUT

Tubesheet layout refers to the configuration of nozzles on the tubesheet. These nozzles are the place of tubes-tubesheet connection. Therefore, their layout depends on position of the tubes. The number of tube passes affects the layout through increasing the number of baffles. This is because an area is needed on the tubesheet to connect the baffles. Among important parameters in tube layouts are the distance between tubes and their angle with each other. There are four tube layout patterns (Figure 2).

- Triangular (30°)
- Triangular (60°)
- Square (90°)
- Square (45°)

The selection of each of these four patterns depends on the settling conditions and other factors, such as pressure drop. The minimum tube pitch is by 1.25 times larger than the tube diameter. In settling processes that need mechanical cleaning, the 90° layout is used. It is worth noting that the triangular (30°) and square (90°) layout patterns accommodate more tubes in the shell.

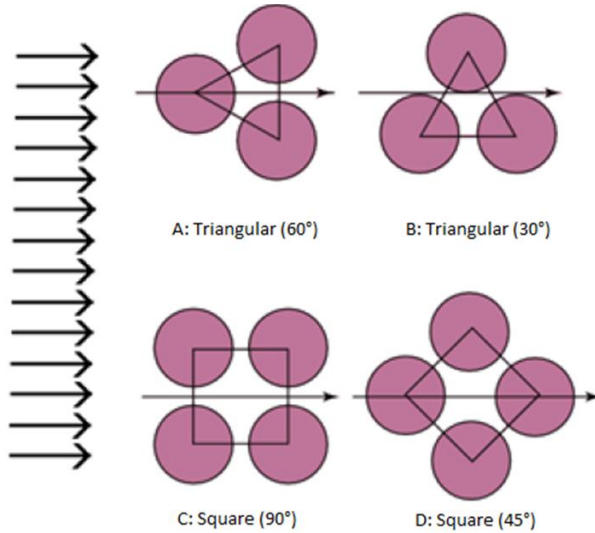


Figure 2. Tube layout in STHES

III. GEOMETRY OF PROBLEM

In this study, four different geometries (cases) were investigated.

Case 1 included circular tubes with 60° triangular layout pattern (Figure 3).

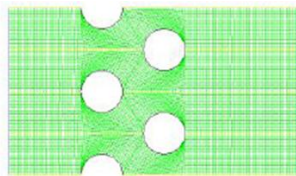


Figure 3. Case 1 with 60° triangular layout pattern

Case 2 included circular tubes with 90° square layout pattern (Figure 4).

Case 3 included elliptical tubes with 90° horizontal square layout pattern (Figure 5).

Case 4 included elliptical tubes with vertical square layout pattern (Figure 6).

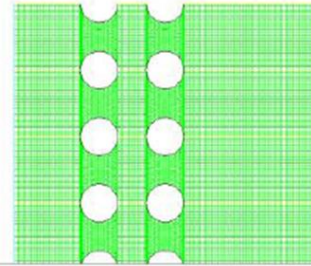


Figure 4. Case 2 with 90° square layout pattern

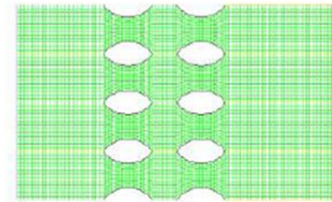


Figure 5. Elliptical tubes of Case 3 with 90° horizontal square layout pattern

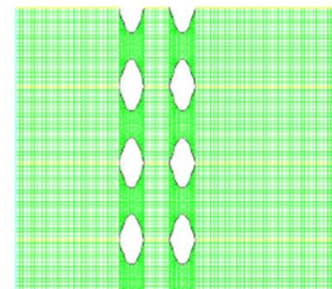


Figure 6. Elliptical tubes of Case 4 with 90° vertical square layout pattern

Dimensions of four prototypes, according to the introduced quantities, are presented in Table 1. According to Figures 3, 4, 5, and 6, the selected geometries for X, Y, and Z axes are introduced along the main flow direction, transverse direction, and perpendicular to the drawing plane, respectively. The velocity components along these directions are u, v, and w, respectively.

A. Meshing

GAMBIT was used for mesh generation. In all four prototypes, a mesh including an organized part with tetrahedral cells and a non-organized part with trihedral cells around the tubes was used. The underlying reason for using this hybrid mesh was that the organized square shape around the tubes reduces the accuracy in that region. In addition, the use of a non-organized mesh is associated with inflated mesh and convergence problems. Meshes in all four prototypes show that they accommodate approximately 200,000 cells.

TABLE I. Pitches of tubes parallel to X-axis and perpendicular to flow direction

Layout	X_L	$P_T = X_t$	Diameter of external tube
	0.704	0.812	0.625
	1.00	1.00	0.750
	0.707	1.00	0.5
	1.25	1.00	0.5

Due to the symmetry of the problem geometry, only one fourth of it is meshed and the boundary conditions of symmetry are applied to side plates.

B. Boundary Conditions

Non-slip conditions ($u=v=w=0$) have been applied to the wall (including tubes and the shell). The temperature of the external wall of the tubes was considered constant (400°K). In addition, the pressure gradient along the normal direction was equated to zero.

In following formula, P is the static pressure and n is the normal direction; in addition, U_∞ is free fluid velocity and T is the static temperature of the input flow.

$$\partial P / \partial n = 0$$

Fluent, as finite-volume based software, was used for computational solution. Due to the large volume of generated meshes and computer memory deficiency, 2D segregated solver with steady-state conditions and implicit solution method with absolute velocity formulation were used. Figure 7 shows a heat exchanger with a fluid pressure inlet defined at its right side and a fluid pressure outlet defined at its left side. Two semicircles, which are defined as wall, indicate thermal springs of the heat exchanger introduced to the problem with higher temperature. The remaining boundaries are defined with symmetry conditions. The shell materials, heated with the fluid inside

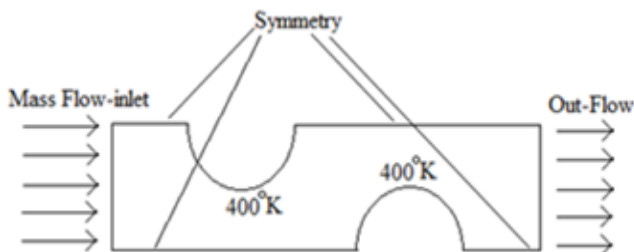


Figure 7. Heat transfer prototype designed in Fluent

the tube, is liquid water with the density of 998.2 Kg/m^3 , specific heat capacity of $C_p=4,182 \text{ j/Kg.K}$, and viscosity of 0.001003 Kg/m.s .

$$C_p=4.182 \text{ j/Kg.K}$$

$$\mu=0.001003 \text{ Kg/m.s}$$

IV. RESULTS

According to Figure 8, the static pressure of fluid inside the shell is more appropriate in Case 2 (90° square layout pattern) and Case 3 (90° square layout pattern of elliptical tubes), rather than other cases. This is because less static pressure is exerted on the shell. In comparison, Case 2 or square layout pattern (90°) is more appropriate than Case 3. Figure 9 compares the pressure exerted on the tubes. According to this figure, less pressure is applied to the tubes in Case 3 (or elliptical tubes) with square layout pattern (90°), preventing damage to them with time.

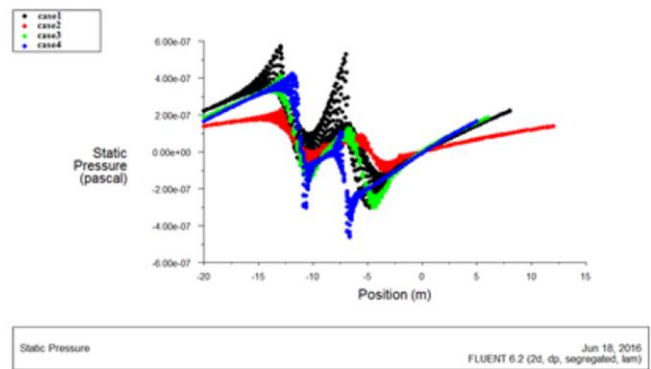


Figure 8. Fluid pressure distribution inside the shell in Cases 1, 2, 3, and 4

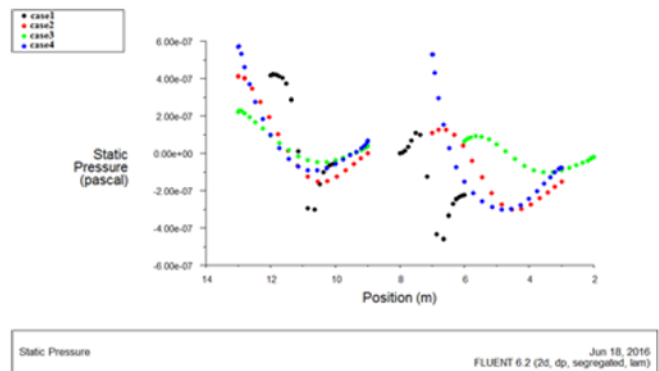


Figure 9. Fluid pressure distribution on tubes in Cases 1, 2, 3, and 4

Figure 10 shows fluid temperature distribution across the shell. According to the diagram, the extents of temperature distribution are very similar in all four methods, but mean high temperature is largely better in Case 1 and Case 2 than other cases. For better detection of temperature distribution, the range of color temperature in each Case can be studied. According to Figure 11, 90° circular tube layout had the most appropriate temperature distribution. Tube layouts can be studied based on the settling in the tube. This can be done by investigating fluid flow lines.

REFERENCES

- [1] Sanaye, S. (2010). Heat Exchangers. Tehran: Iran University of Science and Technology Publishing.
- [2] Clerk Maxwell, A Treatise on Electricity and Magnetism, 3rd ed., vol. 2. Oxford: Clarendon, 1892, pp.68–73.
- [3] Golshahifar, M. (2013). Applied Fluent (ed. 5Th). Tehran: Sanej Press.
- [4] Malekzaded, & Kashanihesar (1957). Designing Heat Exchangers. Jan-e-Farda Publishing
- [5] M Fiebig, N. Mitra, Y. Dong, Simultaneous heat transfer enhancement and flow loss reduction of fin-tubes, Ghetsroni (Ed), Heat Transfer, vol. 3, Hemisphere, Washington, 1990, pp. 51-55.
- [6] M Fiebig, A. Valencia, N. Mitra, Wing-type vortex generators for fin-tube heat exchangers, Exp. Therm. Fluid Sci. 7, 1993, pp.287–295. Article in a journal:
- [7] A. Sohankar, L. Davidson, Effect of inclined vortex generators on heat transfer enhancement in a three-dimensional channel, Numer. Heat Transfer, Part A 39, 2001, pp. 433-448

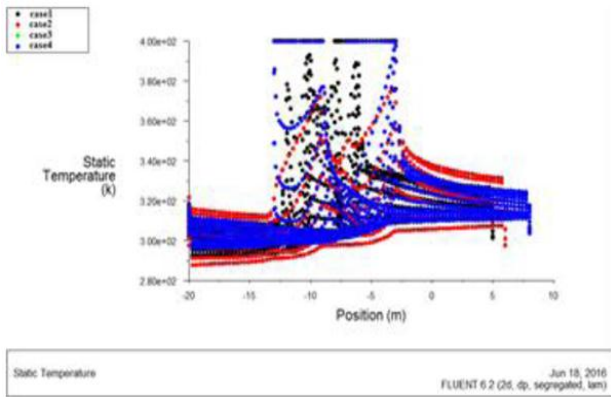


Figure 10. Fluid temperature distribution inside the shell in Cases 1, 2, 3, and 4

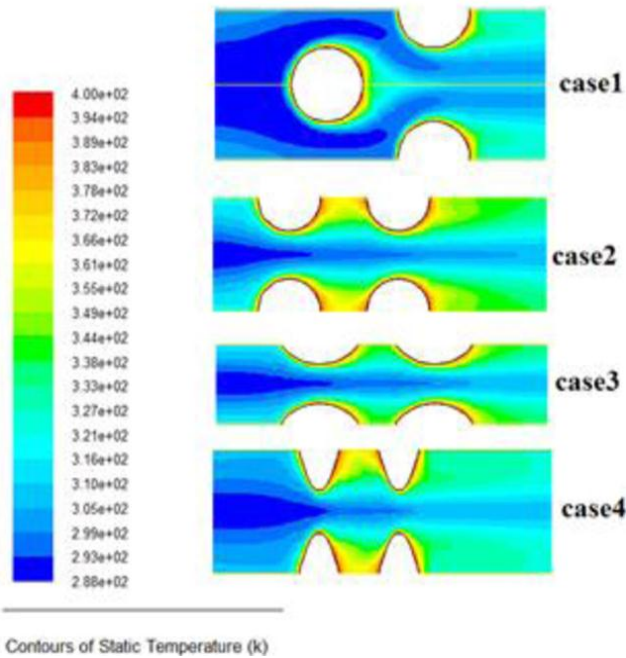


Figure 11. Fluid temperature distribution inside the shell in Cases 1, 2, 3, and 4